Reversal current observed in micro- and submicro-channel flow under non-continuous DC electric field

Yi-fei Duan(段一飞)[1], Hong-wei Ma(马宏伟)[1], Ze-yang Gao(高泽阳)[1], Kai-ge Wang(王凯歌)[1,†], Wei Zhao(赵伟)[1,2], Dan Sun(孙聃)[1], Gui-ren Wang(王归仁)[2], Jun-jie Li(李俊杰)[3], Jin-tao Bai(白晋涛)[1], and Chang-zhi Gu(顾长志)[3]

[1] *State Key Laboratory of Cultivation Base for Photoelectric Technology and Functional Materials, Laboratory of Optoelectronic Technology of Shaanxi Province, National Center for International Research of Photoelectric Technology & Nanofunctional Materials and Application, Institute of Photonics and Photon-Technology, Northwest University, Xi'an* 710069, *China*

[2] *Mechanical Engineering Department & Biomedical Engineering Program, University of South Carolina, Columbia SC* 29208, *USA*

[3] *Laboratory of Microfabrication, Institute of Physics, Chinese Academy of Sciences, Beijing* 100190, *China*

(Received 25 November 2016; revised manuscript received 14 April 2017; published online 20 May 2017)

In practical applications of biochips and bio-sensors, electrokinetic mechanisms are commonly employed to manipulate and analyze the characteristics of single bio-molecules. To accurately and flexibly control the movement of single molecule within micro-/submicro-fluidic channels, the characteristics of current signals at the initial stage of the flow are systematically studied based on a three-electrode system. The current response of micro-/submicro-fluidic channels filled with different electrolyte solutions in non-continuous external electric field are investigated. It is found, there always exists a current reversal phenomenon, which is an inherent property of the current signals in micro/submicro-fluidics Each solution has an individual critical voltage under which the steady current value is equal to zero The interaction between the steady current and external applied voltage follows an exponential function. All these results can be attributed to the overpotentials of the electric double layer on the electrodes. These results are helpful for the design and fabrication of functional micro/nano-scale fluidic sensors and biochips.

Keywords: micro/nano-fluidic channel, reversed-current phenomenon, critical voltage, steady current, overpotential, electric double layer

PACS: 82.45.–h, 73.30.+y **DOI:** 10.1088/1674-1056/26/6/068203

1. Introduction

Micro-nanofluidics have attracted tremendous attentions,[1–4] as they can provide information on single-molecule manipulation and detection,[5–8] medical diagnostics,[9,10] and food safety[11] with high accuracy and throughput. Accompanied with the development of micro-nanofluidic devices, as one of the primary control and detection method, electrokinetic (EK) mechanism are widely used in practice. For example, based on DC electroosmotic flow, DNA and biomacromolecule can be transported in micro-nanochannels for single-molecular analysis.[12] Also, many electric-based techniques, such as impedance spectroscopy, have been developed in biomedical investigations.[13] However, since micro-nanofluidic technology is a multidisciplinary field including physics, chemistry, biomedical engineering, and fluid dynamics, a lot of complex problems are remaining unexplained. Challenges and opportunities coexist. In the investigation of single-molecule, the influence of working conditions, e.g., the diameter of the channel, temperature, pH value, and ionic strength on controlling and detecting macromolecule by EK method is still far from understanding. This could be attributed to either the insufficient accuracy of current detection due to low signal-to-noise ratio (SNR),[14,15] or the contamination and redox products that accumulated on the electrodes that affect the analysis results.[16] Without elucidating the aforementioned problems, analytical devices based on current measurement cannot be an effective way in practical single-molecule applications.

In the meanwhile of studying the EK mechanisms, many other attempts have been made to improve the detection and control on bio-macromolecules. For instance, by the modification of the channel surface, the SNR of micro-nanoscale detectors can be enhanced. People also focused on altering the surface charge characteristics and wettability (hydrophilicity or hydrophobicity) of the inner surface, to realize rapid and accurate analysis on the properties of biological macromolecules, metal particles or polymer molecules.[17,18] Only a few studies have been concerned with the effect of applied

*Project supported by the National Natural Science Foundation of China (Grant Nos. 61378083 and 11672229), the International Cooperation Foundation of the National Science and Technology Major Project of the Ministry of Science and Technology of China (Grant No. 2011DFA12220), the Major Research Plan of the National Natural Science Foundation of China (Grant No. 91123030), the Natural Science Foundation of Shaanxi Province of China (Grant Nos. 2010JS110, 14JS106, 14JS107, and 2013SZS03-Z01), and the Natural Science Basic Research Program of Shaanxi Province — Major Basic Research Project (Grant No. 2016ZDJC-15).

†Corresponding author. E-mail: wangkg@nwu.edu.cn

© 2017 Chinese Physical Society and IOP Publishing Ltd

electrode surface, which should not be neglected. Morrow *et al.*[19,20] theoretically studied the time-dependent development of electric double layer (EDL) in pure water and saline solutions at metal electrode surfaces. They found that the distribution of the electric field and the pH value of the solution near the metal electrodes are seriously influenced by the charges adsorbed onto the top surface of electrode. They also experimentally observed that the current value behaves inversely with the external voltage decays. In 2013, Doi *et al.*[21] experimentally found that as the ionic concentration increases, the transient current signal between the two gold nanoelectrodes decays very slowly and the noise increases gradually. To explain these phenomena, they developed a theory of the ionic current based on the non-equilibrium stochastic model and surficial electrochemical reaction. It is suggested that there exists a fast electrochemical reaction on the surface of electrodes, followed by the slow formation of a diffusion layer. Recently, our investigations have also found that there is a current reverse phenomenon in a three-electrode-pole micro-fluidic system, when non-continuous DC voltage is applied.[22] As the micro-fluidic channels are filled with aqueous solution, the steady current values (I_s) increase from negative to positive with increasing external voltage (U), which means that the direction of current changes. The influence of effective electrode area ratio (γ) between cathode and anode on the reversal current has been studied in details. In the range of γ from 1 to 25, it is found that when the γ is equal to 1 or 4, the steady current value is always positive and increases with the external voltage. When the γ is between 10 and 20, the steady current is negative first and then increased to a positive value at higher voltages. An interesting reversal current phenomenon is observed. We also found that I_s increased with the time interval of pulse voltage and buffer concentration, while it decreased with decreasing pH values of the solution.[23]

For the purpose of accurately manipulating and detecting single biomolecules with micro-nanochannel fluidic technologies, both the principles and the micro-mechanisms of channel-fluidics should be further researched and interpreted in detail from both experimental and theoretical. In this manuscript, we report the characteristics of reversal current signals under a variety of working conditions, e.g., different applied voltage, channel diameter, and ionic concentration of solution. Four kinds of aqueous solutions that commonly used in biological and biomedical circumstance are investigated respectively.

2. Experiments and results

2.1. Experimental setup

The experimental setup is schematically shown in Fig. 1. Two reservoirs that fabricated by polytetrafluoroethylene (PTFE) are connected by a micro-/submicro-channel, to construct the micro-channel system. The micro-channels are fabricated by transparent quartz glass (Beijing Q & Q Technologies Co., Ltd). The inner diameters (d) of the micro-channels are 200 nm, 500 nm, and 5 μm respectively, with the same lengths (L) of approximate 3 mm. Platinum (Pt) electrodes, which has a 0.5-mm diameter and wrapped with 6-mm thick PTFE layer, are applied to measure the ionic current. In addition, the surface area of the counter electrode is much larger than that of the anode to eliminate the effects of polarization. The γ is taken as 20 to investigate the influence of reversal current.[22]

To investigate the current response affected by the working conditions in micro-/submicro-channels the anode (working electrode) and cathode (counter electrode) are placed into two isolated chambers (reservoirs) respectively The one with anode is called *cis* chamber and the other one with cathode is *trans* chamber. A reference electrode is inserted into the *cis* chamber to construct a three-electrode measurement system, instead of the conventional two-electrode measurement system. This can significantly reduce the recovery time of current response, shorten the test time, and improve the experimental efficiency.

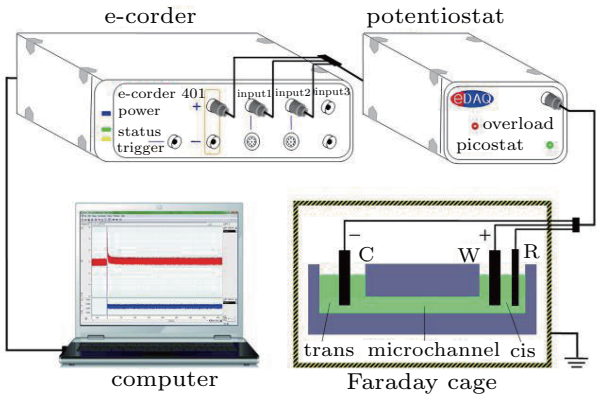


Fig. 1. (color online) Schematic diagram of experimental setup. C, W, and R represent the counter electrode (cathode), working electrode (anode), and reference electrode, respectively. The anode and reference electrode are inserted into the *cis* chamber and the cathode was placed into the *trans* chamber. The micro-current detector and potentiostat are used to detect and record the current signals. The electrode and reservoir system is placed within a Faraday cage.

A high-precision system consisting of a micro-flow potentiostat (pA, EA162, eDAQ, Australia) and a micro-current detector with four-channel data recorder (e-corder 401, eDAQ) is employed to detect the current signals. The software "eDAQ chart" is used to record and analyze the real-time signatures. The sampling frequency is taken as 2 kHz, and the accuracy of current measurement is at the picoampere level. It is worth noting that all of the following experiments are performed when the integrated system of micro-channels and electrodes is placed within a grounded Faraday cage, to perfectly shield the electromagnetic interference.

2.2. Experimental process

The experimental process can be briefly described as below. First, the sample solution is dropped into the *cis* and *trans* reservoirs successively and is induced to move through the micro-channel with capillary force. This operation is performed very carefully to ensure that no bubbles or contamination particles are introduced into the channel. Second, place the entire micro-fluidic channel platform in the Faraday cage. Insert the anode and reference electrode into the *cis* chamber, and the cathode into the *trans* chamber. Finally, an appropriate voltage is applied between the two electrodes. The ions are transferred through the micro-channel under the electric field. In the meantime, the real-time current signals are recorded.

During the experiments, under each external voltage, the current signal is consistently recorded for 10 minutes, until the current reached a steady state. Then, the DC electric field is turned off. After 2 minutes, turned on the DC electric field and started another measurement. To eliminate contamination, the reservoirs and channels are dipped into deionized water (DI water) for approximately 1 hour and then cleaned with an ultrasonic cleaner for 10 minutes before starting a new measurement. The electrodes are also cleaned by the ultrasonic cleaner. All of the experiments are carried out at 25 °C.

The detailed experimental information is listed in Table 1.

Table 1. Experimental conditions.

Parameters	Value
Solution type	DI water, TBE, KCl, Tris
Voltage/mV	0–500 (increasing and decreasing)[a]
pH	2, 4, 7, 9, 11
Concentration/M	0.2, 0.5, 1.0
Channel diameter/μm	0.2, 0.5, 5

[a] 'increasing' represents the voltage changing from 0 mV to 500 mV and 'decreasing' is in the opposite process.

3. Results and discussion

3.1. Reversed-current phenomenon

When aqueous solution was driven to move within the micro-nanofluidic channel by an external electric field, it was generally found with increasing applied voltage, the current values of the steady state turned from negative into positive, or changed from positive into negative. A reversed current phenomenon can be found. The phenomenon and related critical voltage are tightly related to the experimental conditions we investigated. The results are introduced and discussed below.

3.1.1. Reversal current signal

Figure 2 shows typical current signals under various applied voltages, when KCl solution (0.05 M, pH = 7) is filled in the micro-channel with a diameter of 5 μm.

In Fig. 2(a), it can be clearly observed that under 10 mV, the current had a greater positive value initially, followed by a quickly decreasing. After a few seconds, a steady state was achieved. The steady current I_s was negative at approximately −3.8 nA. When the external voltage is 20 mV, the current signal exhibits a larger initial value and a positive steady state at 1.6 nA. Furthermore, when the external voltage was increased to 40 mV, the initial current becomes even larger. The steady state current is 4.1 nA. The current always exhibits larger value in the initial phase, and then quickly decreased to a steady state as shown in Fig. 2(a).

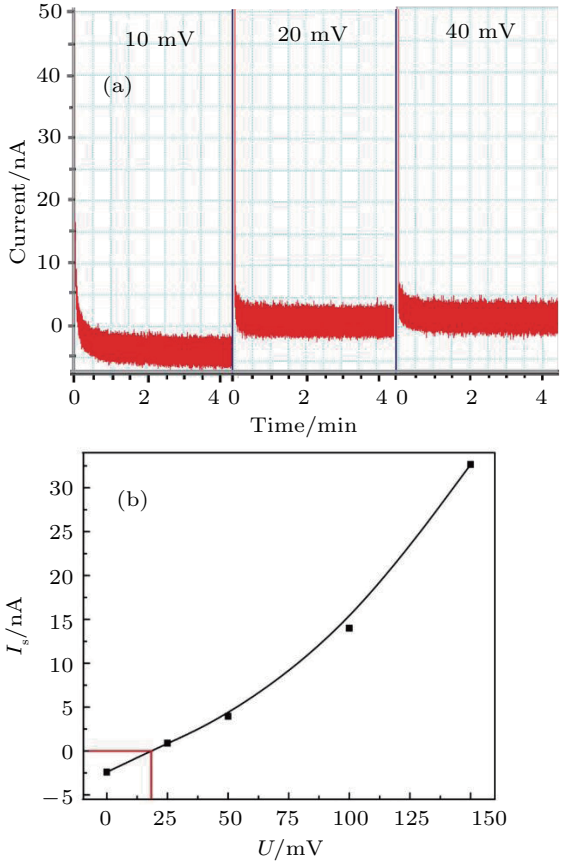


Fig. 2. (color online) Current value curve with time, 0.05-M KCl solution, pH = 7, diameter of channel $d = 5$ μm. (a) The current decays with time. Pausing about 2 minutes between 10 mV and 20 mV, and 20 mV and 40 mV. (b) The relationship between steady state current and external applied voltage. The solid line is curve fitted.

The variation of steady state currents (I_s) with applied voltage (U) is plotted in Fig. 2(b). When U is lower than a critical voltage (U_c), i.e., 18 mV, the steady current I_s is negative. The current is in the opposite direction of the external voltage. When U is larger than 18 mV, the I_s becames positive, i.e., in the same direction of the external voltage. Besides, generally say, I_s increases U monotonically. The relation between the steady current I_s and external applied voltage U, as shown in Fig. 2(b), can be approximately expressed by an exponential function as follows:

$$I_s = a \cdot e^{-U/k} + b, \tag{1}$$

where a and b are constants and k is the decay constant. By nonlinear fitting, it is found, $a = 0.18517$ nA, $b =$

-0.23497 nA, and $k = -126.12436$ mV, respectively. The exponential model shows good consistency with experimental measurements.

3.1.2. Typical current response

Figure 3 displays the six typical current signals recorded during the experiments.[22] These six typical current signals can be attributed to two different mechanisms, depending on the applied parameters.

As shown in Figs. 3(a), 3(b), 3(d), and 3(e), initially, the magnitudes of currents increases rapidly to a peak value. After that, the current magnitude monotonically decreases with time respectively. The evolution of current can be divided into three stages: (i) initiation stage; (ii) attenuation stage; and (iii) steady-state stage. This phenomena was also observed by Morrow and McKenzie,[19] as soon as the power source was switched on. They attributed this phenomenon to the necessity of time cost to achieve the applied voltage value. However, their theory cannot explain the peak of current. Actually, the current characters shown in Figs. 2(a) and 3 can be better understood with the overpotential theory[24] and the EDL theory[25] in the three-electrode monitoring system.

During the experiments, the Pt electrodes will be polarized so long as there is electric current passing through the electrodes, which produces overpotentials on the electrodes. The potentials of the electrodes will exhibit deviation from the original equilibrium one (φ_r). The potential of the cathode is lower than that of the theoretical equilibrium value ($\varphi_c = \varphi_r - \varphi_{over}$), and the anode potential is larger than the anode potential at theoretical equilibrium ($\varphi_a = \varphi_r + \varphi_{over}$), where φ_c is the potential of cathode, φ_a is the potential of anode, and φ_{over} is the overpotential. This deviation from the equilibrium electrode potential is defined as the overpotential (Pt), and therefore the practical electrode potential is not equal to the theoretical value.

Generally say,[26] overpotentials can be grouped into three categories: activation, concentration, and resistance. Since Pt electrodes have very stable physical and chemical properties, the activation overpotentials around the interface of Pt electrodes are negligible.[27] Therefore, the overpotentials around the interface of Pt electrodes are primarily determined by the concentration and resistance overpotentials.[28] Both of them can results in a peak current: the former one can generated peak current by polarization overpotential, while the latter one is always accompanied with the peak current in the "switch on" process. Since in the experiments, the measurement is normally conducted after the electrodes was immersed in the solution, the initial polarization has been finished. Therefore, the peak current should be aualitatively dominated by the resistance overpotentials.

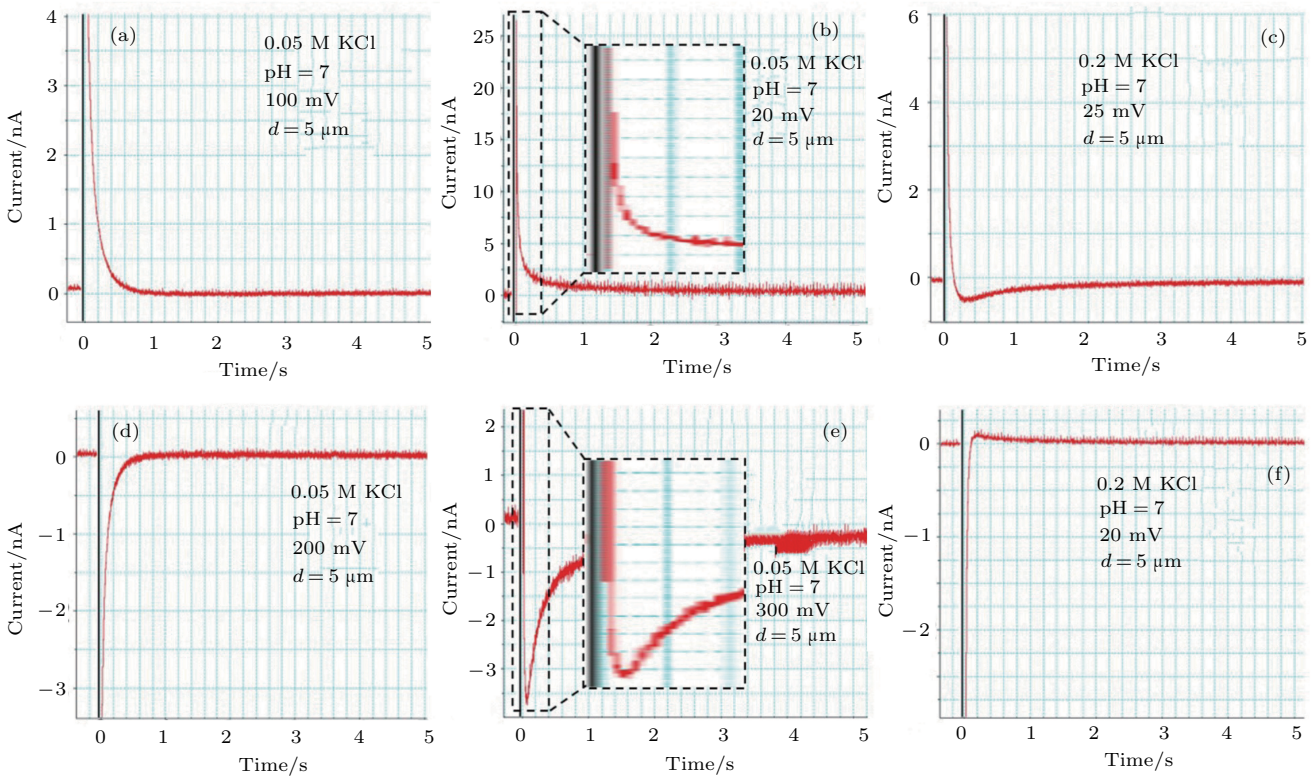


Fig. 3. (color online) Typical models of current signal curves at the initial stage. The current signals in panels (d), (e), and (f) are the reversal response of panels (a), (b), and (c), respectively. [(a) and (b)]: A typical exponential decay of I, where 0.05-M KCl, external voltage is 100 mV, 20 mV, respectively, pH = 7, the channel diameter is $d = 5$ μm. (c): A typical oscillating decay of I, where 0.2-M KCl, at 25 mV, and pH = 7, $d = 5$ μm. [(d) and (e)]: A typical exponential decay of $|I|$, where 0.05-M KCl, external voltage is 200 mV, 300 mV, respectively, and pH = 7, $d = 5$ μm. (f): A tyical oscillating decay of $|I|$, where 0.2-M KCl, external voltage is 20 mV, pH = 7, $d = 10$ μm.

If the initial overpotential is not sufficiently strong (probably due to the low ionic concentration), after the peak current is generated, a screening region will be formed gradually by the accumulation of these opposing charges near the electrodes. This screening region is also denoted as the EDL of the electrode pole.[27] Then, a shield electric field (E_{opp}) along the micro-channel in the opposite direction to the external electric field (E_o is established. The slowly increasing accumulation of charges causes stronger shielding field E_{opp}. Consequently, the actual electric field intensity ($E_o - E_{opp}$) between the two electrodes gradually decreases, and the current is reduced with the square root of time as described by the Cottrell equation:[29] $I(t) = nFSC_R\sqrt{D_R/\pi t}$, where n is the number of electrons transferred per molecule, F is the Faraday constant, S is the area of the electrode surface, C_R is the concentration of the reduced species R, and D_R is the diffusion coefficient of R. Eventually, the charges accumulated on the two electrode surfaces will achieve a saturation state, and so does the current.

While 0.2-M KCL solution is applied, the monotonic decaying process is replaced by an turn-over decaying process, as plotted in Figs. 3(c) and 3(f). Probably due to the higher concentration, a larger initial overpotential and faster charge accumulation can be predicted. A strong E_{opp} is generated. While the overpotential is finished, the external electric field is not sufficiently strong to overcome the high E_{opp}. The overall electric field intensity will be in the direction of E_{opp} and opposite to the external electric field. The turn-over phenomenon of current can be observed.

3.1.3. The probability of the six typical current response

The six typical current response occurs not certainly in the measurements, but probably. Therefore, statistical analysis were proceeded on the 6 typical current signals to evaluate the probability of each case. The experiments were conducted in both 5-μm and 10-μm micro-channels. In the 5-μm micro-channel, a total of 273 measurements that show negative Is are statistically investigated. While in the 10-μm micro-channel, 353 measurements are statistically investigated. The probability histograms are plotted in Fig. 4.

From Fig. 4, it can be observed:

(i) In the 5-μm micro-channel, among the six types of current signals, the phenomenon shown in Fig. 3(a) has the highest probability upto 69.96%. The curves shown in Fig. 3(d) has less chances at 27.11%. Relatively, the total probability of both Figs. 3(c) and 3(f) are 0.3662%.

(ii) In the 10-μm micro-channel, the probability of case (a) is decreased, while the probabilities of other cases are increased. The overall probability related to monotonic decaying process is slightly decreased in the 10-μm micro-channel, and the corresponding decaying process with turn-over phenomenon becomes more observable. Or in other words, in the micro-channel with smaller diameter, the turn-over phenomenon of current becomes rare and the current is more "controllable".

Since the movement of bulk ions in our micro-channel system is primarily determined by three mechanisms, which are electrophoresis, electroosmotic flow and diffusion. Both the electrophoresis and diffusion are dominated by the length scale of micro-channel, not the diameter. Only the electroosmotic flow is strongly affected by the diameter of micro-channel. At the initial stage, due to overpotential, the EDL moves faster than at the steady state. And so does the bulk flow (out of EDL) of EOF. After the overpotential is finished, the steady state voltage cannot provide such a fast EOF, and there exists a deceleration of EDL. The EDL can be decelerated immediately due to electric field, but the bulk flow and the related ions movement cannot respond immediately. This may induce a disordered EOF, and the corresponding lag or oscillation of ion transport. In a smaller micro-channel, due to the stronger influence of viscosity, the ions movement in bulk flow can be decelerated faster than in a larger micro-channel. Therefore, the convective transport of ions by the inertial effect of bulk flow can be more controllable in smaller micro-channels and prohibit the generation turn-over phenomenon of current. This could explain why in the 10-μm micro-channel, the occurrence probability of decaying process with turn-over phenomenon is higher.

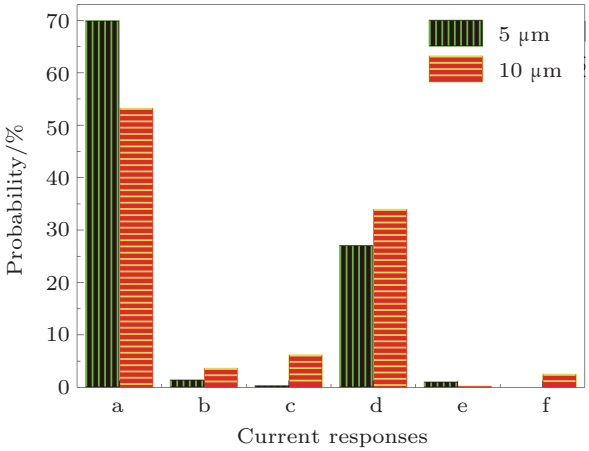


Fig. 4. (color online) Histograms of the probabilities of six typical current signals corresponding to Figs. 3(a)–3(f) respectively. The green histograms with vertical stripes represent the probabilities of six current signal in the micro-channel with 5-μm diameter, and the orange histograms with horizontal stripes are for the 10-μm diameter micro-channel.

3.2. The influence of control parameters

In this section, all of the control parameters, e.g., electrolyte of solution, external applied voltage, ionic concentration, pH value, and inner diameter of the channel, were systematically studied.

3.2.1. The electrolyte of solution

To investigate whether the current-reversal phenomenon occurred in a particular aqueous solution, four kinds of solutions were compared, which are DI Water, KCl (1.0 M), Tris (10 mM), and TBE. The TBE buffer is composed of Tris (hydroxymethyl) aminomethane, boric acid (Borate), and disodium ethylene diamine tetraacetic acid (EDTA-2Na) in a certain proportion. At the concentration of 1× TBE, the concentration of Tris (hydroxymethyl) aminomethane, boric acid (Borate), and EDTA-2Na are 0.09 M, 0.09 M, and 0.002 M respectively.

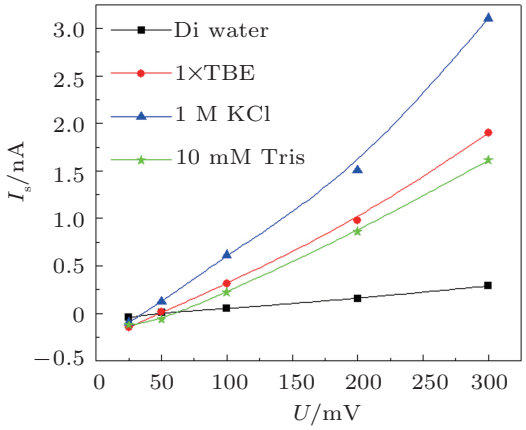


Fig. 5. (color online) Steady current values of four solutions varying with external applied voltage. ■, ●, ▲, and ⋆ represent DI water, 1× TBE, 1-M KCl, and 10-mM Tris, respectively. Diameter $d = 5$ μm.

Figure 5 shows the steady current values for the four aqueous solutions under 0 mV to 300 mV. It can be clearly seen, initially, all of the steady current values were negative. The currents increased gradually with voltage with different slopes. Due to the different initial steady current values and slopes of I_s–U curves, the critical voltages in the four cases were 47 mV, 73 mV, 60 mV, and 94 mV, respectively. From Fig. 5, the phenomena of current reversal were observed in all the four aqueous solutions in the 5-μm diameter microchannel driven by an electric field force. This indicates that the current-reversal phenomenon is not belong to a specific solution, but commonly existed.

3.2.2. Applied voltage and the operation sequence

To investigate the influence of the external applied voltage and its operation sequence on the current-reversal phenomenon, two kinds of voltage operation sequences were systematically studied as a comparison. That is, the external applied voltages were set to either increase from 0 mV to 400 mV or decrease from 400 mV to 0 mV.

In Fig. 6, the variations of steady current with voltage under different operation sequences are plotted, for all the four aqueous solutions. A hysteresis phenomenon can be found when changing the operation sequence. When a larger external voltage is applied, the difference of current values in different operation sequence becomes larger too. It is also found: 1) For each solution, the I_s–U curve basically follows the exponential relationship in Eq. (1), no matter in which operation sequence; 2) The U_C value in the increasing process was a little bit larger than that of the decreasing process, i.e. there is hysteresis phenomenon between the two operation sequences.

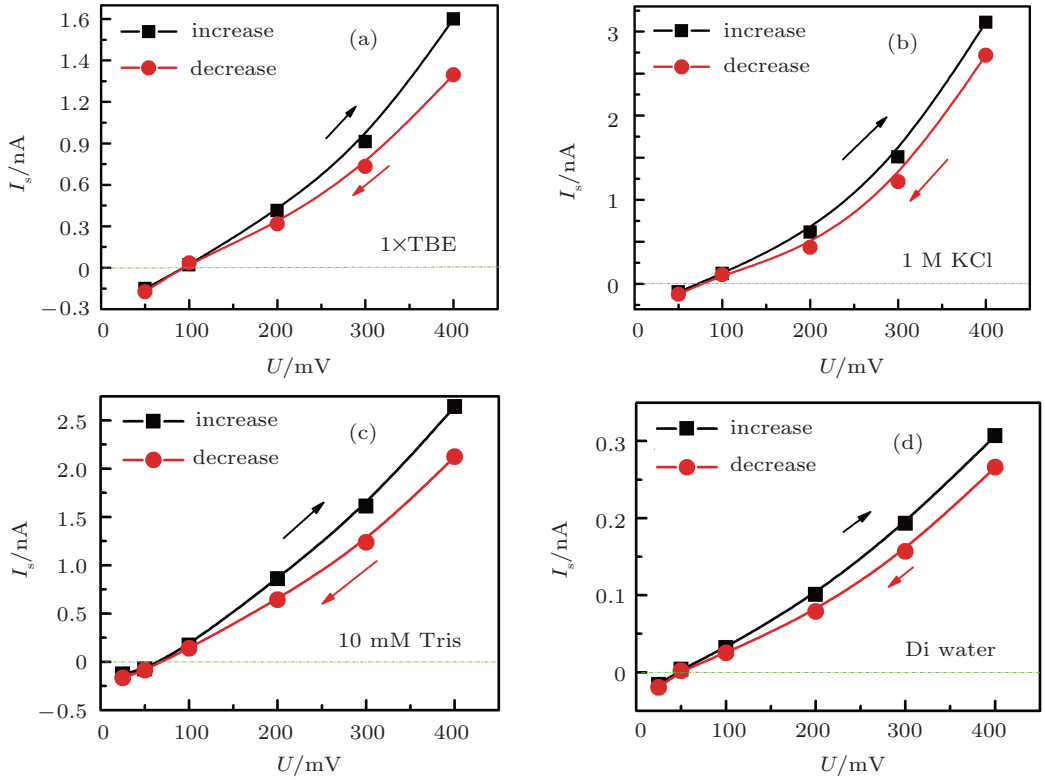


Fig. 6. (color online) Steady current varying with external applied voltage. ■ and ● represent the applied voltage change sequence for an increasing and decreasing process, respectively. (a) 1× TBE, (b) 1-M KCl, (c) 10-mM Tris, and (d) DI water. Diameter $d = 5$ μm.

The hysteresis of current can be attributed to the charge accumulation on electrode surface. When the applied voltage was increased, more charges were accumulated on the electrode surface. An equilibrium state of electric field in micro-channel is rapidly established. While the applied voltage was decreased, the surface charges cannot stay around the electrodes and diffused back to the bulk solution. However, since the charge accumulation on the electrode surfaces that determined by electrostatic force is much faster than that of ions diffused back to bulk solution (on the time scale of 10^3 s–10^4 s), much more time is required to establish a new equilibrium state. The residue charges around electrodes generate opposite electric field relative to the applied external one. It results in a smaller overall electric field in the micro-channel, and so does the smaller current values. This is why hysteresis phenomenon of current can be observed.

Consequently, the U_C of the increasing sequence was smaller than that of the decreasing process, as shown in Table 2. For the four solutions, i.e., 1× TBE (Fig. 6(a)), 1-M KCl (Fig. 6(b), 10-mM Tris (Fig. 6(c), and DI water (Fig. 6(d), U_C in the increasing process were 92, 73, 66, and 47 mV, respectively, while the U_C in the decrease process were 94, 76, 69, and 48 mV, respectively. However, the difference is very small. The relative difference is no more than 4.5% in all the four cases. Therefore, the operation sequence of applying voltage should not have a significant effect on the measurement of current reversal phenomenon.

Table 2. Critical voltages under the two opposite operation sequences of the voltage.

Solution	Increasing/mV	Decreasing/mV	Critical voltage (U_c)		Percentage[a]/%
			Difference/mV	Average/mV	
1× TBE	92	94	2	93	2.15
1-M KCl	73	76	3	74.5	4.03
10-mM Tris	66	69	3	67.5	4.44
DI Water	47	48	1	47.5	2.11

[a] percentage = $\left|\text{difference}/\text{average}\right| \times 100\%$.

3.2.3. Ionic concentration

Case (a): In 5 μm micro-channel

KCl electrolyte with various concentrations was selected to investigate how the current-reversal phenomenon was affected by the ionic concentration. The experiments were conducted in the 5-μm micro-channel.

Figure 7(a) shows the I_s–U relations under different ionic concentrations by ensemble averaging. Since in single-biomolecule detection, the buffer concentration is usually lower than 1 M, the selected ionic concentrations were 0.2 M, 0.5 M, and 1.0 M, respectively. It can be seen, in all the three concentrations, the initial current values are negative. As the concentrations of KCl aqueous solution is increased, i.e., 0.2 M, 0.5 M, and 1.0 M, the values of U_c in the increasing process of applied voltage were 52, 31, and 20 mV, respectively. Therefore, with increasing ionic concentration of the KCl solution, the critical voltage was reduced, which revealed that the screening electric field produced was smaller with larger ionic concentration.

Case (b): 500-nm-diameter channel

The influence of the KCl concentration on the current-reversal phenomenon is also investigated in the 500-nm channels, as shown in Fig. 7(b). Three concentrations of the KCl solution are considered, which are 0.2 M, 0.5 M, and 1.0 M, respectively.

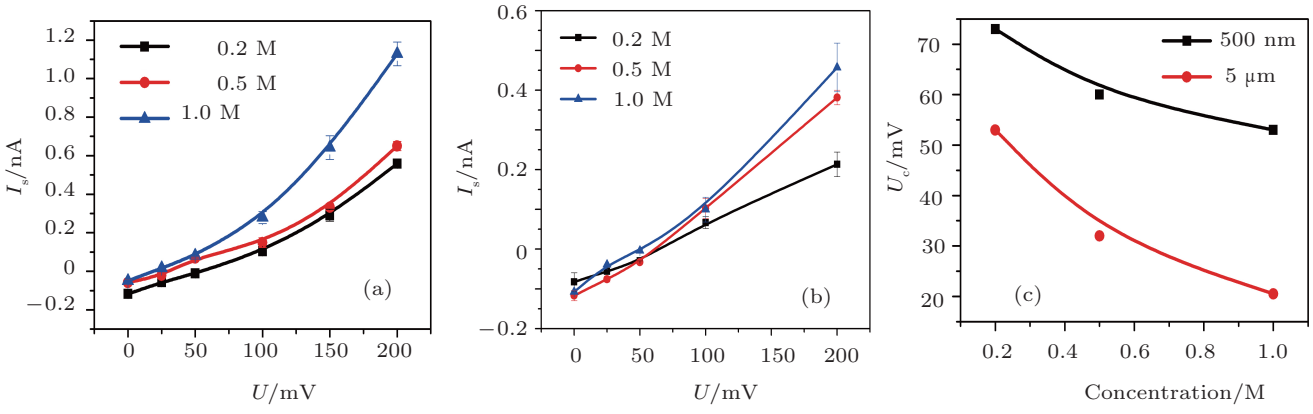


Fig. 7. (color online) The ensemble averaging steady current versus applied voltage and the corresponding critical voltages, for various ionic concentrations of KCl solution. Here, pH = 6. (a) I_s–U relation in 5-μm micro-channel. (b) I_s–U relation in 500-nm submicro-channel. (c) The relation between ionic concentration and critical voltage in the channels with different diameter.

It can be seen, the I_s–U relation is less exponential at lower concentrations. At the concentration of 0.2 M, the I_s–U relation approaches approximately linear. As the concentration is increased, the I_s–U becomes consistent with the exponential equation (1) $I_s = a \cdot e^{-U/k} + b$. For each working condition, I_s was negative at the beginning and then reversed to a positive value as the voltage is increased.

Case (c): UC versus ionic concentration

The relations between critical voltages and concentrations in the two channels are plotted in Fig. 7(c). It can be seen in both cases, the critical voltage U_c decreased with increasing concentration (C) of solution. In the meanwhile, at same concentration, the critical voltages in 500-nm channel is always higher than in the 5-μm channel. The influence of channel diameter will be discussed in details later.

The main reason for this phenomenon could also be the electrical double layer (EDL) on the electrodes. The EDL thickness (Debye length) is thinner at higher ion strength and thicker at lower ion strength, and the strength of the screening electrical field increases with increasing EDL thickness. The thickness of EDL changes with the ionic concentration.[30,31] For a monovalent electrolyte at 25 °C (298 K), the Debye length (k^{-1}, k is the Debye–Hückel parameter) of the aqueous solution can be described with the following equation:[32] $k^{-1} = 3.04 \times 10^{-10}/\sqrt{C}$. where C is the solution concentration. For the solution with same ions, when the solution concentration is lower, the thickness of the EDL of the electrode surface is greater and the zeta-potential is higher.[33] The shielding field caused by the accumulated charges is stronger. As a result, a great amount of applied voltage is required to counteract the effect of the shielding field, and the critical voltage U_c is larger.

3.2.4. Solution pH

In the practical applications of micro-nanofluidic technology, especially for studying single biological molecules, the pH value of the solution is a critical factor. For example, the pH value of buffer solution is usually set as alkalescent environment to ensure the activity of DNA molecules.

Figure 8 shows how the steady current value and the critical voltage are affected by pH values. During our experiments, the pH values of solutions, such as pH = 2, 4 (acidic), pH = 9, 11 (alkali), as well as the neutral condition pH = 7, were selected. Extreme conditions such as pH = 1 or 12 were not chosen because these values are not commonly used in practical applications and may damage the electrode.

It can be seen in Fig. 8(a) that under different pH values, all the I_s–U curves matches well with Eq. (1), despite the different fitting coefficients. The steady currents were first negative and then reversed to positive as the external applied voltage is increased. The critical voltage U_c was not a constant, but decreased with the increasing pH value by a linear relationship approximately, as shown in Fig. 8(b). This could be attributed to the charges absorbed onto the electrode surface[24,25] and induce different surficial potential which were significantly affected by the pH value. In principle, once a solid-oxide material is immersed into electrolytic solution, the solid-liquid surface then forms an electrically charged layer. This layer can be due to two mechanisms:[34,35] (a) amphoteric dissociation of surface MOH groups, i.e., $MOH \rightarrow M^+ + OH^-$ or $MOH \rightarrow M^- + H^+$; (b) adsorption of metal hydroxo complexes derived from the hydrolysis products of material dissolved from the solid, i.e., from amphoteric dissociation of $M^{2+}(OH_2^-$. Here, M stands for a metallic element. Both mechanisms can partially qualitatively explain the relationship between the pH value and surface charge.

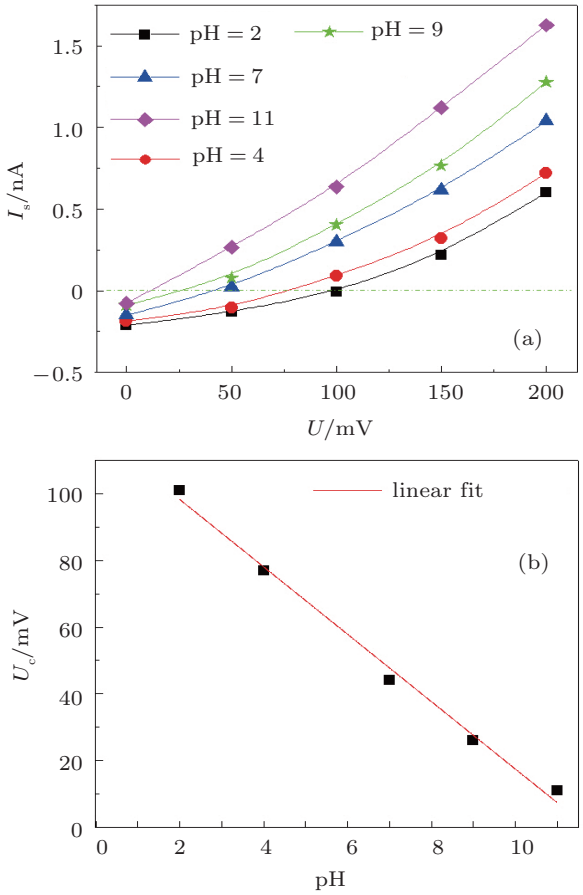


Fig. 8. (color online) (a) Steady current versus applied voltage under various pH values. (b) Critical voltage versus pH value. 1.0-M KCl solution. $d = 5$ μm.

When the amount of net surface charge is equal to zero, the pH value is defined as the isoelectric point (IEP) or the zero point of charge (ZPC).[36] The ZPC has been widely employed to indicate that there is no surface charge of a metal oxide immersed into solution, or to reveal that the concentrations of the anion and cation of hydroxyl complexes are

equal and electrically neutral. During our experiments, when the platinum (Pt) electrode was immersed into the electrolytic solution, there was a chemical reaction equilibrium between the metal (Pt) and metal oxide (PtO) on and near the electrode surface. The reaction can be described by the following equation:[37,38] $Pt + 2H_2O = PtO + 2H^+ + 2e$. Kruyt *et al.*[39] has found that the ZPC of PtO is approximately equal to 14. Thus, it can be reasonably speculated that the net charge adsorbed onto the electrode surface should be reduced as the pH value increases Recently, Morrow and McKenzie[19] found that in pure water, a large number of anions were gathered around and onto the anode and then the nearby hydronium ions (H_3O^+) were consumed. This increases the local pH value. In the meanwhile, the H_3O^+ surrounding the cathode resulted in the environmental pH value decreasing. They have also observed that both the maximum and minimum pH value on each electrode linearly changed with the external applied voltage. Therefore, it can be inferred that because of the influence of solution pH, the adsorption ability of the anode surface is weaker than that of the cathode, and the amount of surface charge on the anode is lower than that on the cathode.

3.2.5. Size of channel diameter

In micro-nanofluidics, as the inner diameter of channel is decreased, the surface-to-volume ratio increases. The scale effect and surface effect becomes stronger.

To evaluate the role of the channel diameter on the current-reversal phenomenon, three channel diameters, i.e., 200 nm, 500 nm, and 5 μm, were employed. Figure 9 shows the I_s–U relations in 0.5-M and 1-M KCl electrolytes in the three channels. From Fig. 9(a), it can be seen that in the channels with diameters of 200 nm, 500 nm, and 5 μm, U_c of 0.5-M KCl solution were 123 mV, 60 mV, and 30 mV, respectively. While, for the 1-M KCl solution as shown in Fig. 9(b), U_c were 116 mV, 51 mV, and 20 mV respectively. Apparently, the critical voltages decrease with the increasing channel diameter. This implies the influence of surface electrochemistry becomes important.

This might be related to electroosmosis,[40,41] since electroosmotic flow can cause an opposite convection of ions and inhibit the ions transport by electrophoresis. With the decreasing of the channel diameter, the electroosmotic flow might be strengthened; thus, to counter balance the opposite electric field, the external electric field needs to be comparatively stronger. As a result, the U_c increases with the decreasing diameter of the channel. The U_c in 10-μm micro-channel was also studied. Since the critical voltage is negligibly affected by the solution concentration, the data is not shown.

From Fig. 9, it can be clearly observed that, no matter what the size of the channel diameter is, the current-reversal phenomena occurred in all the investigated cases. Also, the variations of the steady current versus applied voltage were highly similar and consistent with Eq. (1). For the 500-nm-diameter channel: $a = 0.11634$ nA, $b = -0.35934$ nA, and $k = -110.54472$ mV, while for the 200-nm-diameter channel: $a = 0.10392$ nA, $b = -0.34016$ nA, and $k = -105.8402$ mV. These results indicate that the current-reversal phenomenon was not occasionally occurs in a particular channel.

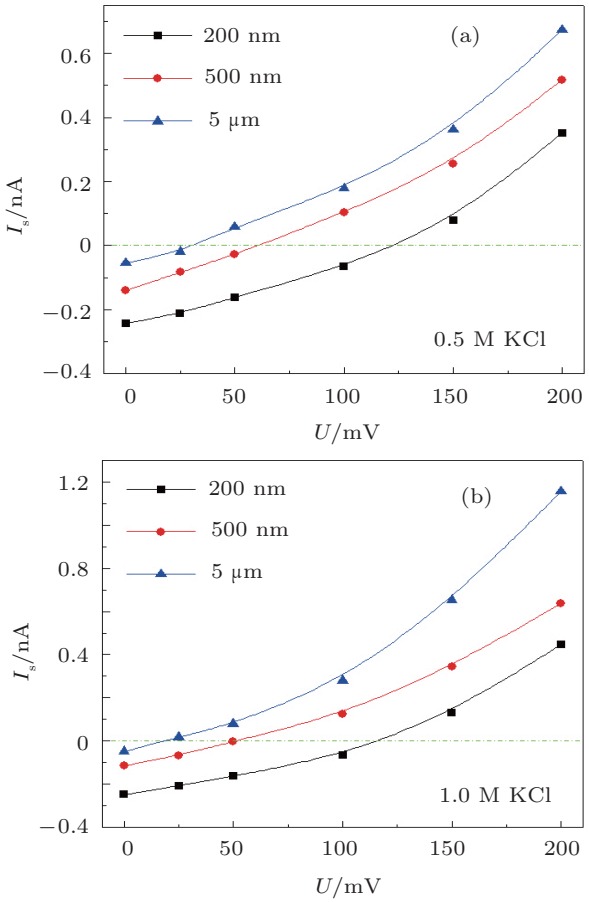


Fig. 9. (color online) Steady current versus voltage for various channel diameters. The concentrations of the electrolyte KCl are (a) 0.5 M and (b) 1 M. ■, ●, and ▲ represent channel diameters of 200 nm, 500 nm, and 5 μm, respectively.

4. Conclusion

In this paper, the influences of electrolyte, concentration of solution, pH value and the diameter of channel on critical voltages of reversal current have been parametrically investigated in details. Four solutions which are DI water, Tris, TBE, and KCl are investigated.

Six typical current responses to external voltage are first studied and their occurrence are attributed to the overpotential and EDL formed on the electrodes. Then, the reversal current is found to be an inherent phenomenon when the γ is beyond 5. It is also found: (I) The operation sequence of applied voltage has negligible influence on the measured critical voltages; (II) With increasing ionic concentration of the solution, the critical

voltage was reduced; (III) The critical voltage decreased with the increasing pH value by a linear relationship approximately; (IV) In micro-nanofluidics, the critical voltage decreased with the increasing of inner diameter of channel.

The current response, no matter the instantaneous one at the initial stage or the steady one, is crucial on the application of electric methods in micro-nanochannels, especially when the applied voltage is small. The investigation can deepen our understanding on the electric features of micro-nanochannel. Based on the current-reversal phenomenon, novel micro-nanofluidic devices can be designed for flexible and accurate controlling and detection. This is especially useful for manipulating single biomolecules and other dispersed phases in biomedical and chemical applications.

Acknowledgments

The authors are grateful to Fengyun Yang and Shuang Wang for their help on guidance of the instrument and discussion.

References

[1] Sang S, Feng Q, Tang X, Wang T, Huang X, Jian A, *et al.* 2015 *Microelectron. Eng.* **134** 33
[2] Sang S, Zhao Y, Zhang W, Li P, Hu J, Li G 2014 *Biosensors and Bioelectronics* **51** 124
[3] Wang H W, Bao N, Le T T, Lu C, Cheng J X 2008 *Opt. Express* **16** 5782
[4] Yang F Y, Wang K G, Sun D, Zhao W, Wang H Q, He X, *et al.* 2016 *Chin. Phys. B* **25** 525
[5] Streets A M, Huang Y 2014 *Current Opinion in Biotechnology* **25** 69
[6] Mawatari K, Pihosh Y, Shimizu H, Kazoe Y and Kitamori T 2013 "Micro and Extended-Nano Fluidics and Optics for Chemical and Bioanalytical Technology", *Progress in Nanophotonics* 2 (Springer) p. 121
[7] Wang K G, Yue S, Wang L, Jin A, Gu C, Wang P Y, *et al.* 2006 *Microfluidics and Nanofluidics* **2** 85
[8] Arnold S, Holler S and Fan X 2015 "Taking Microcavity Label-Free Single Molecule Detection Deep into the Protein Realm: Cancer Marker Detection at the Ultimate Sensitivity", *Nano-Structures for Optics and Photonics* (Springer) p. 309
[9] Rivet C, Lee H, Hirsch A, Hamilton S and Lu H 2011 *Chem. Eng. Sci.* **66** 1490
[10] Yang A H and Erickson D 2008 *Nanotechnology* **19** 045704
[11] Atalay Y T, Vermeir S, Witters D, Vergauwe N, Verbruggen B, Verboven P, *et al.* 2011 *Trends in Food Science & Technology* **22** 386
[12] Zhang B, Wood M and Lee H 2009 *Anal. Chem.* **81** 5541
[13] Katz E and Willner I 2003 *Electroanalysis* **15** 913
[14] Mathwig K and Lemay S G 2013 *Micromachines* **4** 138
[15] Zevenbergen M A G, Wongrajit N, Singh P S, Goluch E D, Wolfrum B L, Lemay S G, *et al.* 2010 *Electrochemical Nanofluidics: The mesoscopic limit Rsc Org*
[16] Myers F B and Lee L P 2008 *Lab on a Chip* **8** 2015
[17] Tabard-Cossa V, Trivedi D, Wiggin M, Jetha N N and Marziali A 2007 *Nanotechnology* **18** 305505
[18] Marie R, Beech J P, Vörös J, Tegenfeldt J O and Höök F 2006 *Langmuir* **22** 10103
[19] Morrow R and McKenzie D (eds.) 2011 "The time-dependent development of electric double-layers in pure water at metal electrodes: the effect of an applied voltage on the local pH", *Proc. Roy. Soc. Lond. A: Math., Phys. and Eng. Sci.* (The Royal Society)
[20] Morrow R, McKenzie D and Bilek M 2006 *J. Phys. D: Appl. Phys.* **39** 937
[21] Tsutsui M, Ohshiro T, Chien C C, Zwolak M, Taniguchi M, Kawai T, *et al.* 2013 "Electrochemical response of biased nanoelectrodes in solution", arXiv: 13023016
[22] Ma H W, Wang K G, Gao Z Y, Wang H Q, Wang S, Zhang C, *et al.* 2014 *AIP Adv.* **4** 107139
[23] Gao Z Y, Wang K G, Zhang C, Ma H W, Wang G R and Bai J T 2014 *Sci. China-Technol. Sci.* **57** 249
[24] Wang D Y and Nowick A S 1979 *J. Electrochem. Soc.* **126** 1166
[25] Hittorf W 1853 *Annalen der Physik* **165** 177
[26] Bard A J, Faulkner L R, Leddy J and Zoski C G 1980 *Electrochemical methods: fundamentals and applications* (New York: Wiley)
[27] Matyushov D V 2009 *J. Chem. Phys.* **130** 234704
[28] https://en.wikipedia.org/wiki/Overpotential
[29] Girault H H 2004 *Analytical and Physical Electrochemistry* (CRC Press)
[30] Schoch R B, Han J and Renaud P 2008 *Rev. Mod. Phys.* **80** 839
[31] Plecis A, Schoch R B and Renaud P 2005 *Nano Lett.* **5** 1147
[32] Israelachvili J N 2011 *Intermolecular and surface forces*, rev. 3rd edn. (Academic Press)
[33] Li D Q 2004 *Electrokinetics in Microfluidics*, Vol. **2** (Elsevier Academic Press)
[34] Parks G A and Bruyn P D 1962 *J. Phys. Chem.* **66** 967
[35] Yopps J and Fuerstenau D 1964 *Journal of Colloid Science* **19** 61
[36] Parks G A 1965 *Chem. Rev.* **65** 177
[37] Kinoshita K and Madou M 1984 *J. Electrochem. Soc.* **131** 1089
[38] Li J P, Peng T Z and Lin Y H 2002 *Chin. J. Anal. Chem.* **30** 670
[39] Kruyt H R, Jonker G and Overbeek J T G 1952 *Colloid Science, Irreversible Systems* **1**
[40] Rathore A S 2002 *Electrophoresis* **23** 3827
[41] Seiler K, Fan Z H, Fluri K and Harrison D J 1994 *Anal. Chem.* **66** 3485